

lecture 13.1.2011

we had so far:

- binding in clusters and their appearances in mass spectra
 - a) undirected van-der-Waals bonding
 - b) ionic bonding
 - c) covalent bonds

today:

- d) metallic bonding

Mackay icosahedra

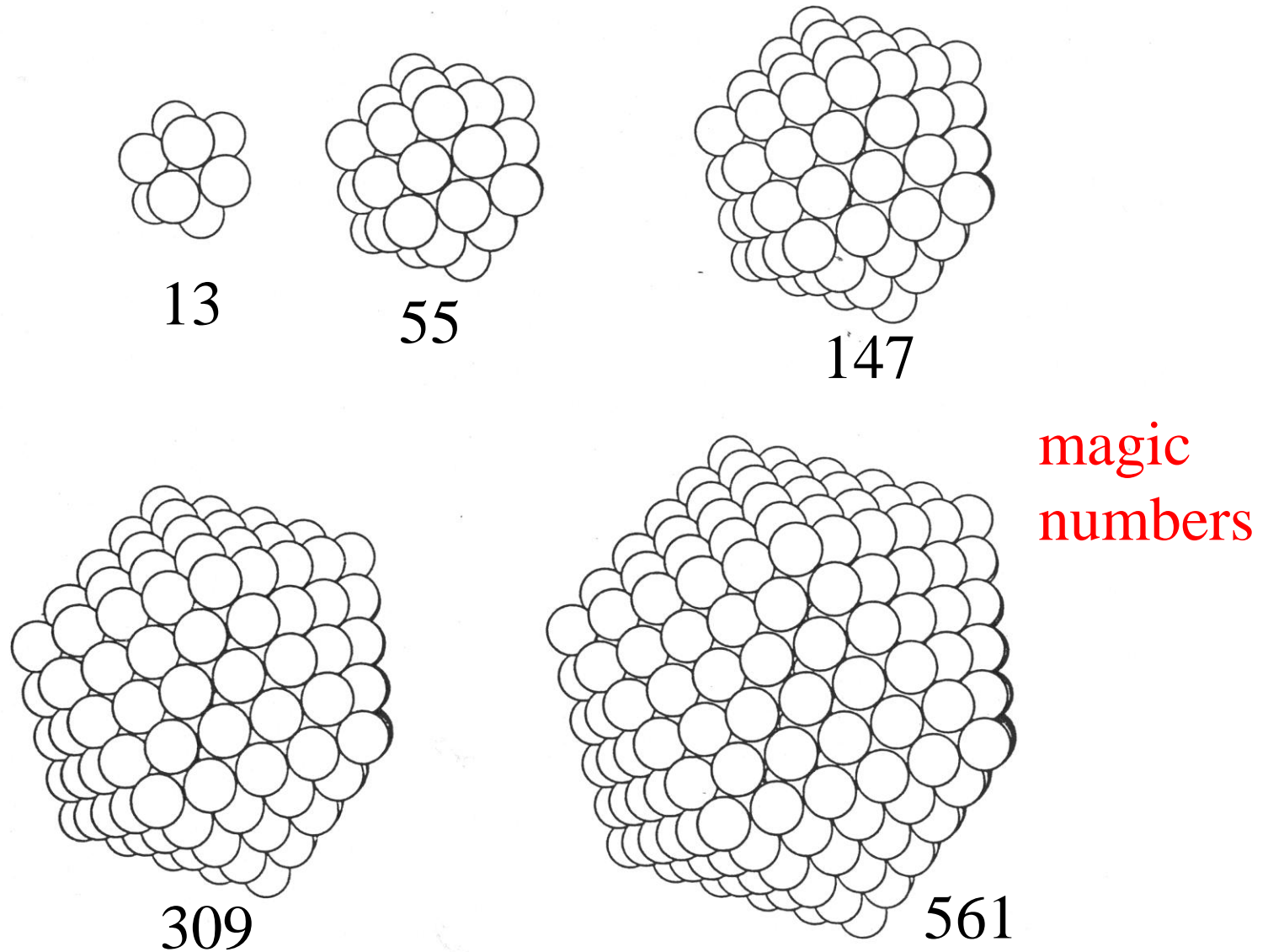
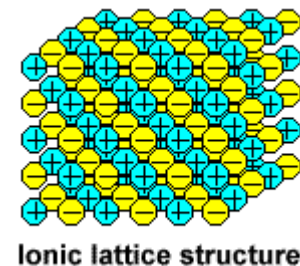
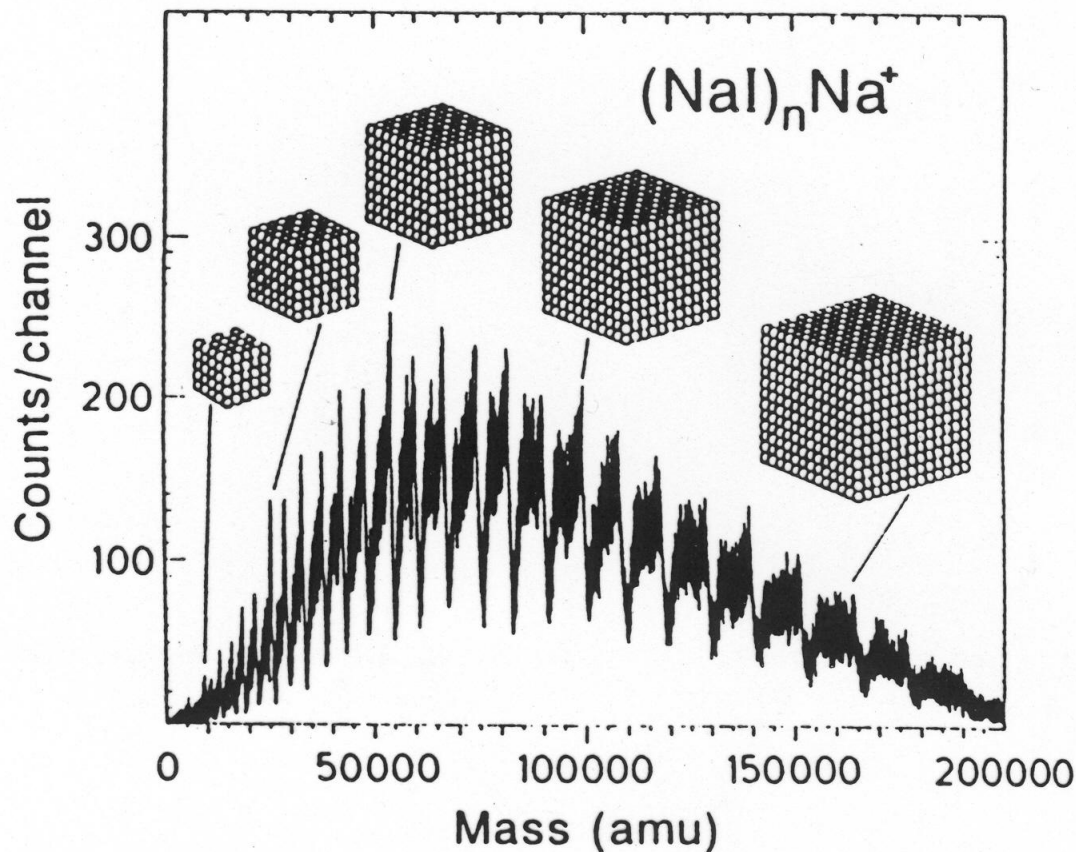


Fig. 5. The first five Mackay icosahedra. $N = 13, 55, 147, 309,$ and $561,$ respectively.

ionic bonding in alkali halides



T.P. Martin

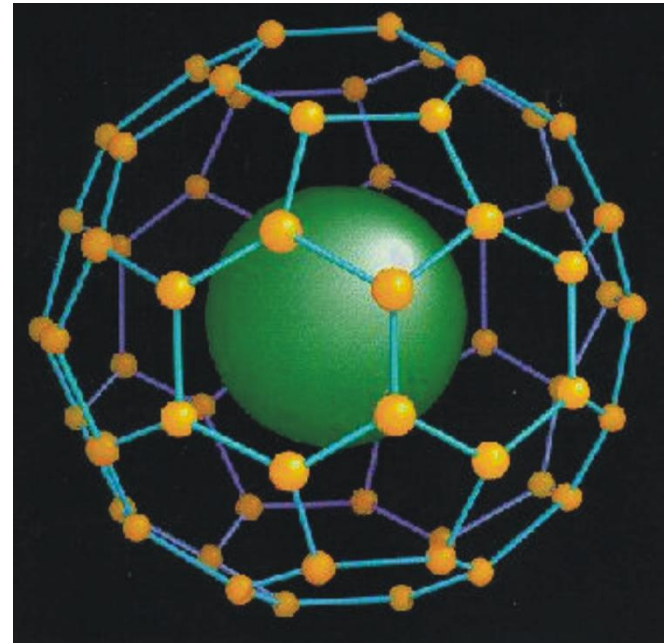
Fig. 5. Mass spectrum of $\text{Na}(\text{NaI})_n^+$ clusters. The interval between the oscillations corresponds to the number of atoms needed to cover one face of cuboid-shaped clusters.

covalent bonds: Buckminster-Fulleren



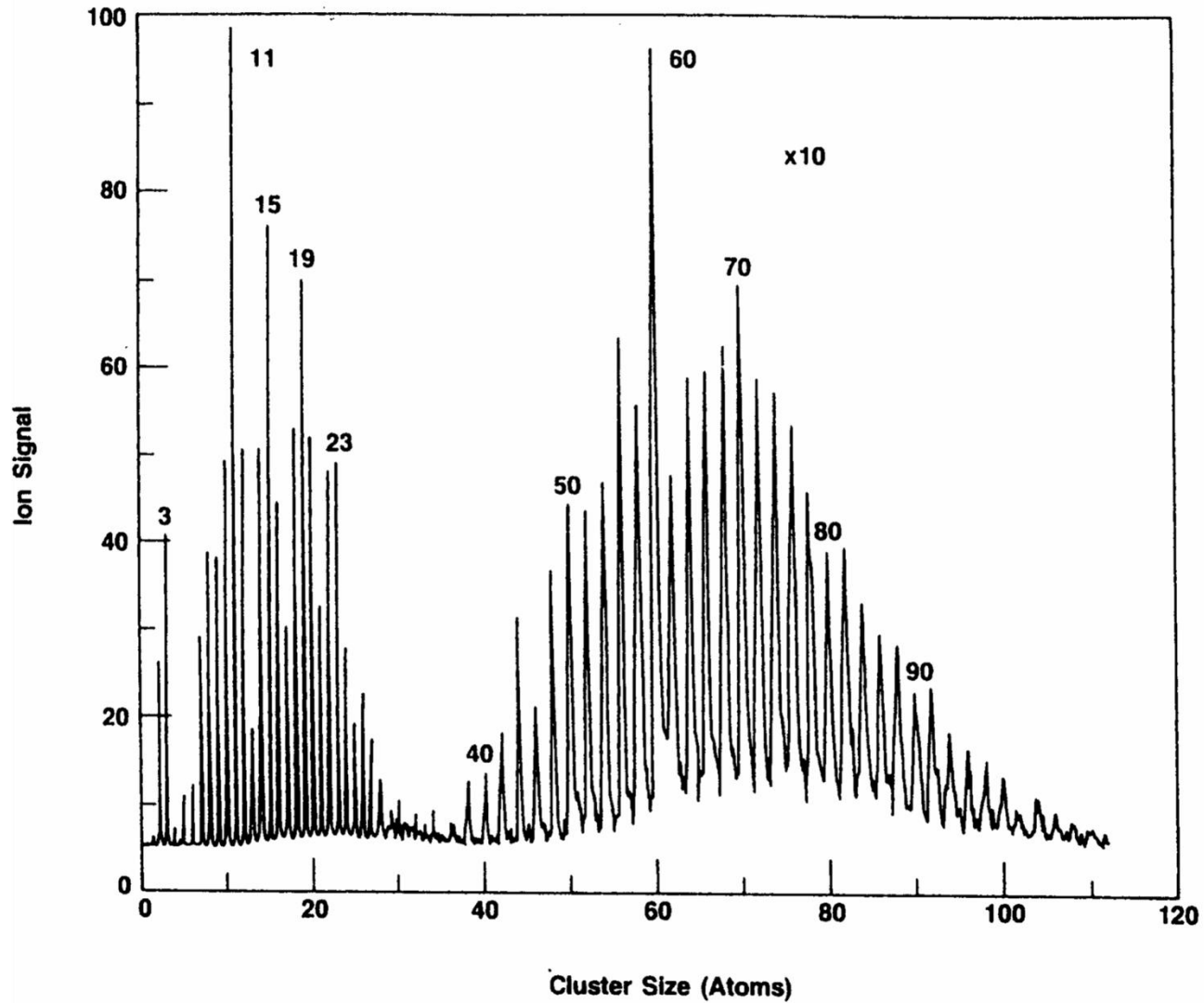
C_{60}

"Buckminster-Fulleren"



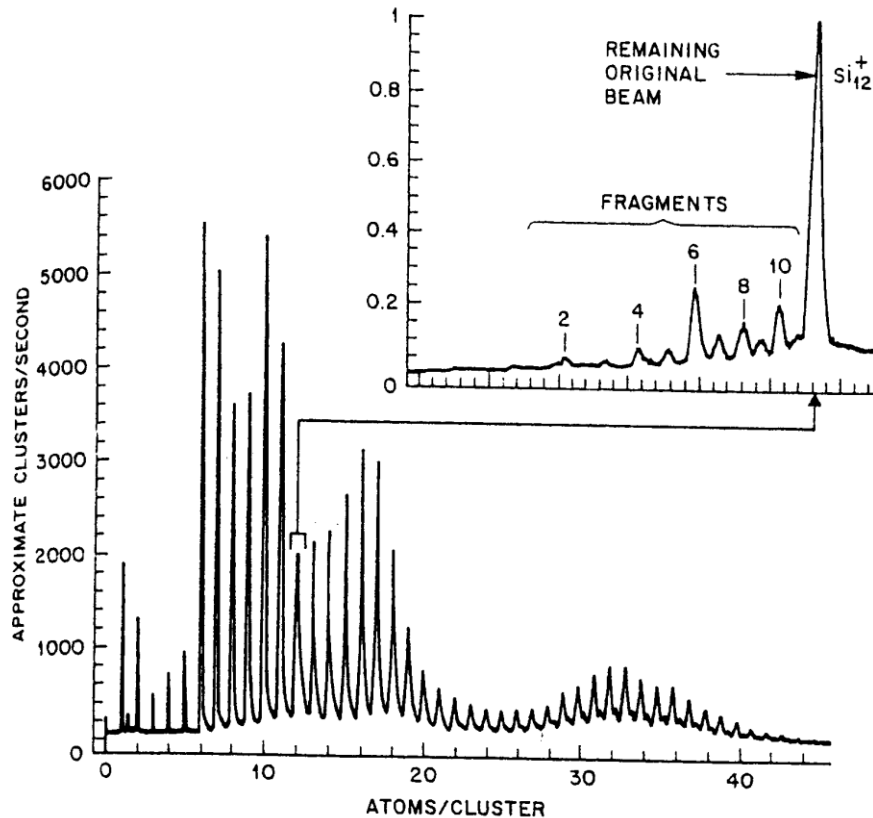
Lanthan Atom in C_{60}

mass spectrum of carbon clusters



mass spectra of silicon clusters

Charged clusters show magic number $n=6, 10, 16$ and 32 , but a maximum in the spectrum is not followed by a deep minimum for $n+1$ atoms ! (Photofragmentation shows no monomer evaporation).



binding in clusters

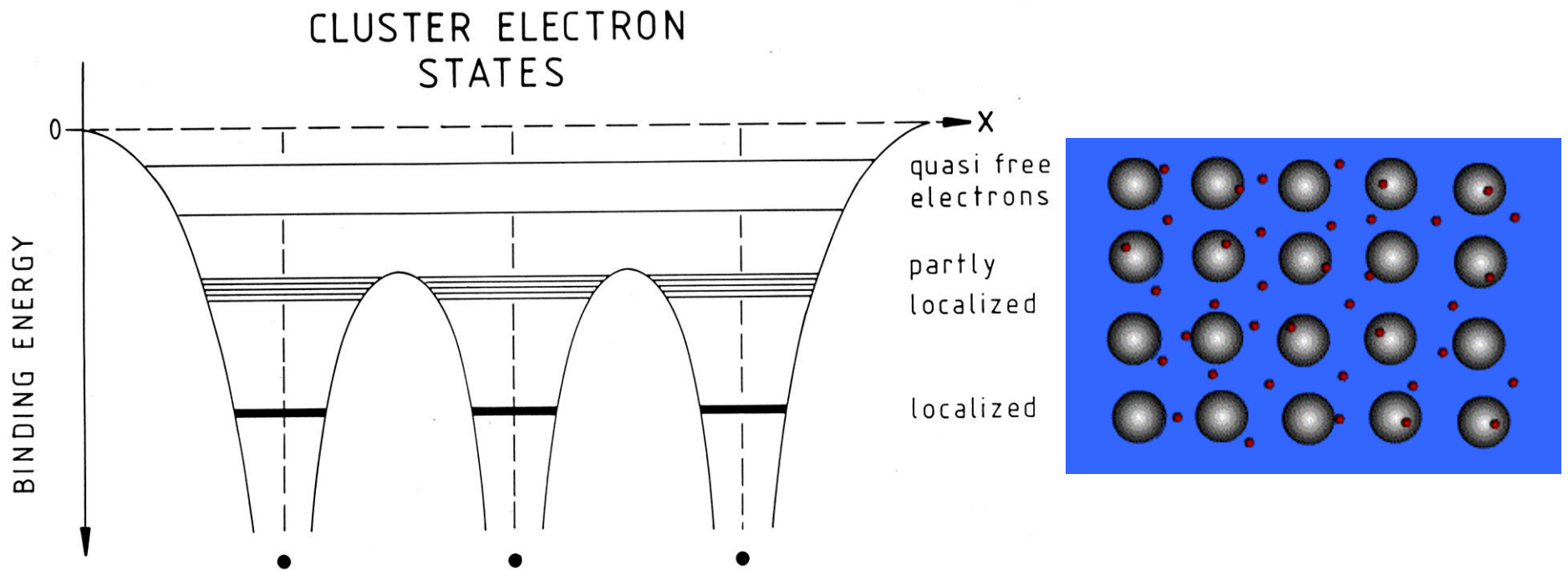
a) undirected bonding (Van-der-Waals)

b) ionic

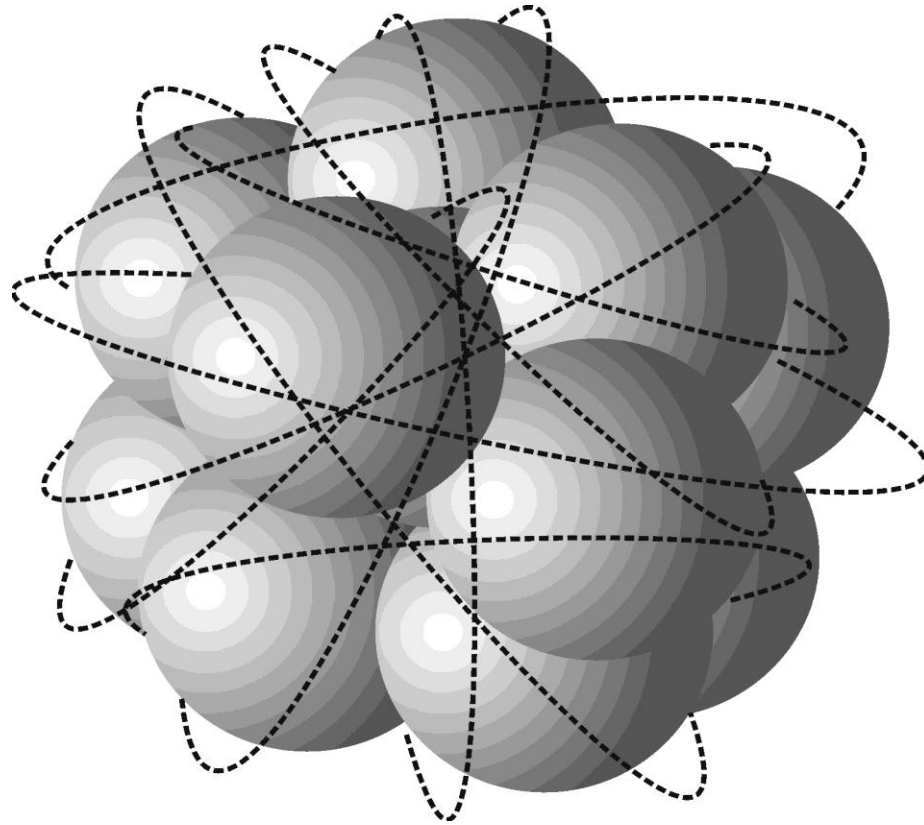
c) covalent

d) metal bonding

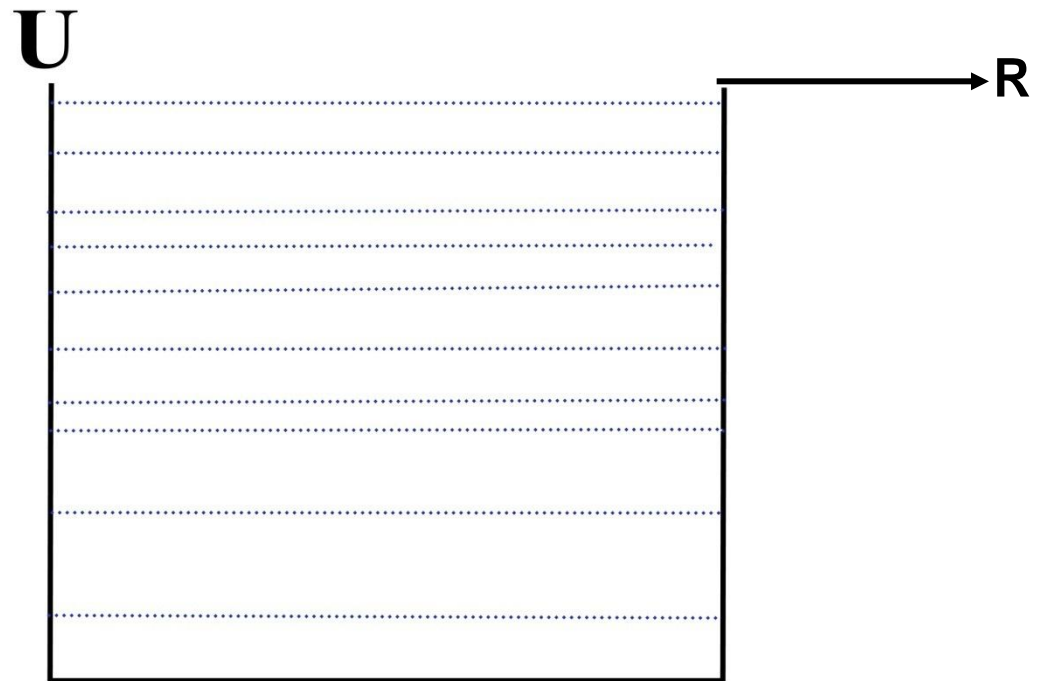
Schematics of metal binding in a cluster



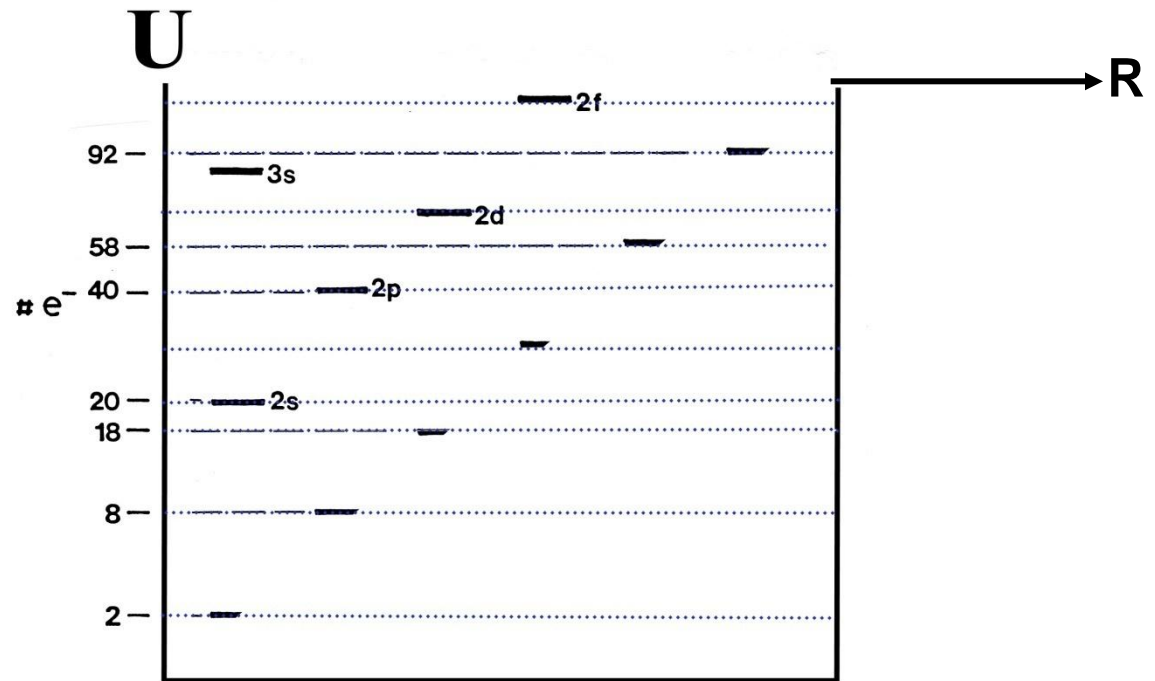
A cluster of simple metal atoms can be considered as a metallic quantum dot. In the corresponding bulk materials the electrons need much more space.



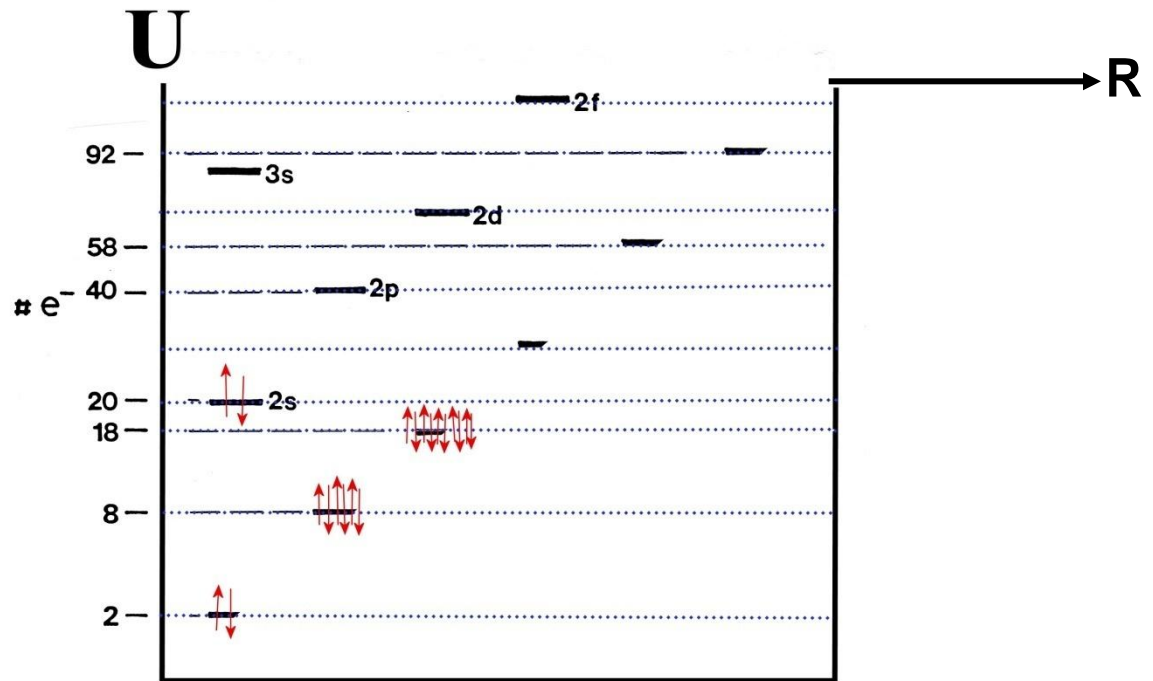
The spherical jellium model: basic idea



The spherical jellium model: basic idea



The spherical jellium model: basic idea



c.f. nuclear physics

Woods Saxon potential

compare: potential energy function for atomic nucleus

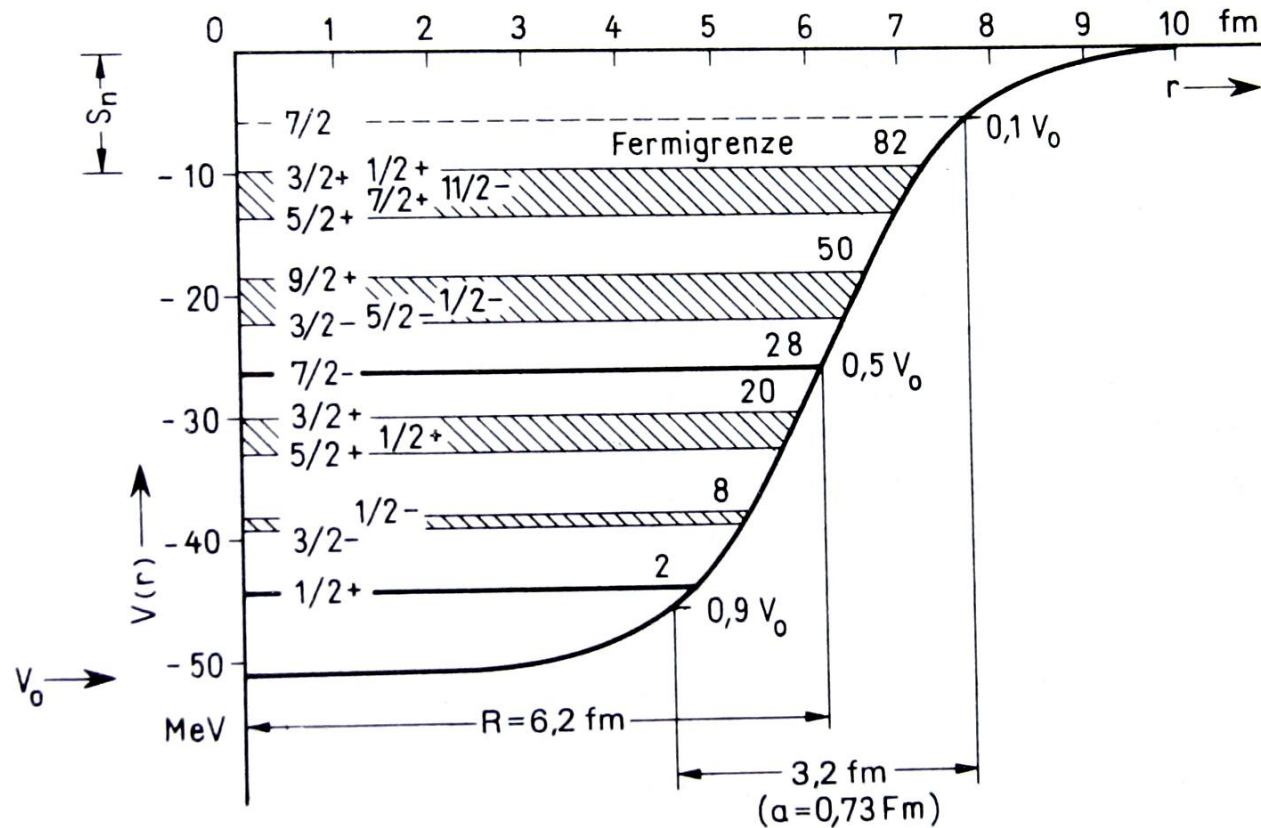
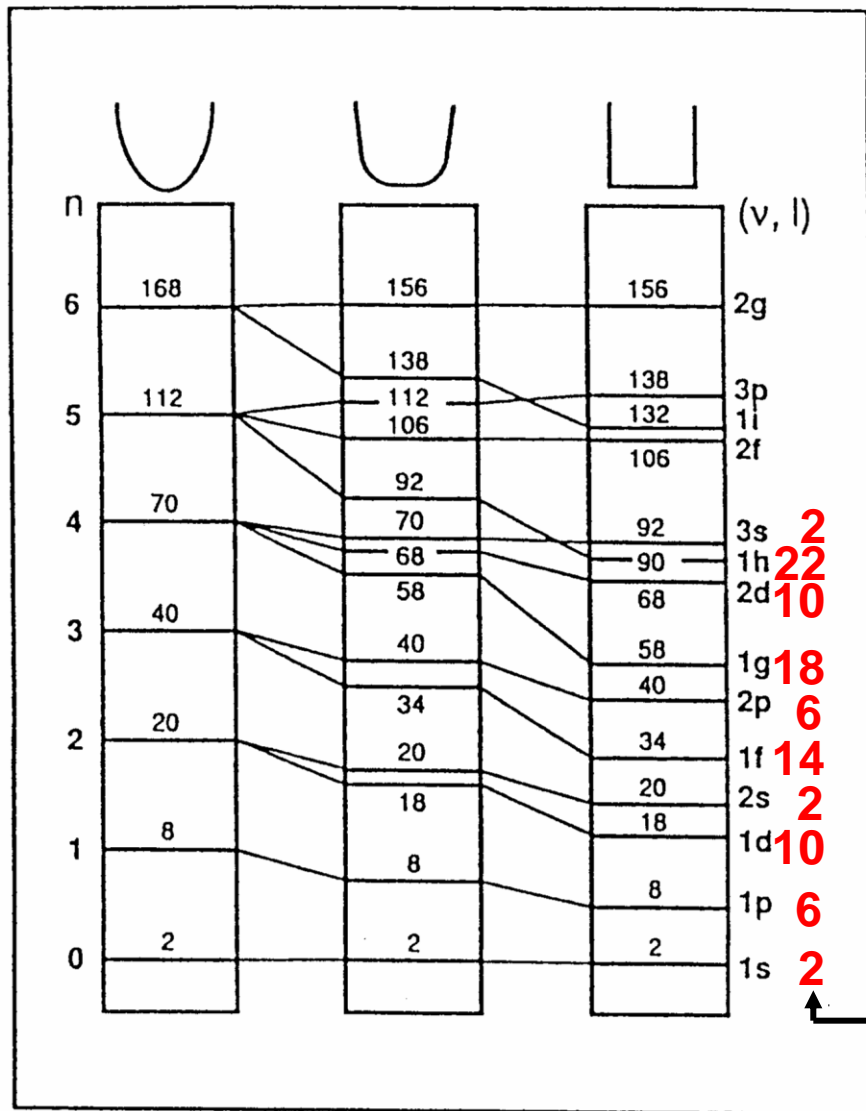


Fig. 81 Realistische Darstellung der Verhältnisse beim Schalenmodell. Neutronenniveaus eines Kerns mit $N=80$ im Kernpotential; R und a sind Parameter des Woods-Saxon-Potentials Gl. (6.8); nach [Bei 64]

The spherical jellium model: role of the potential like in *nuclear physics*



Explains the magic numbers of neutral alkali clusters :
2, 8, 20, 40, 58, 70, 92 ...

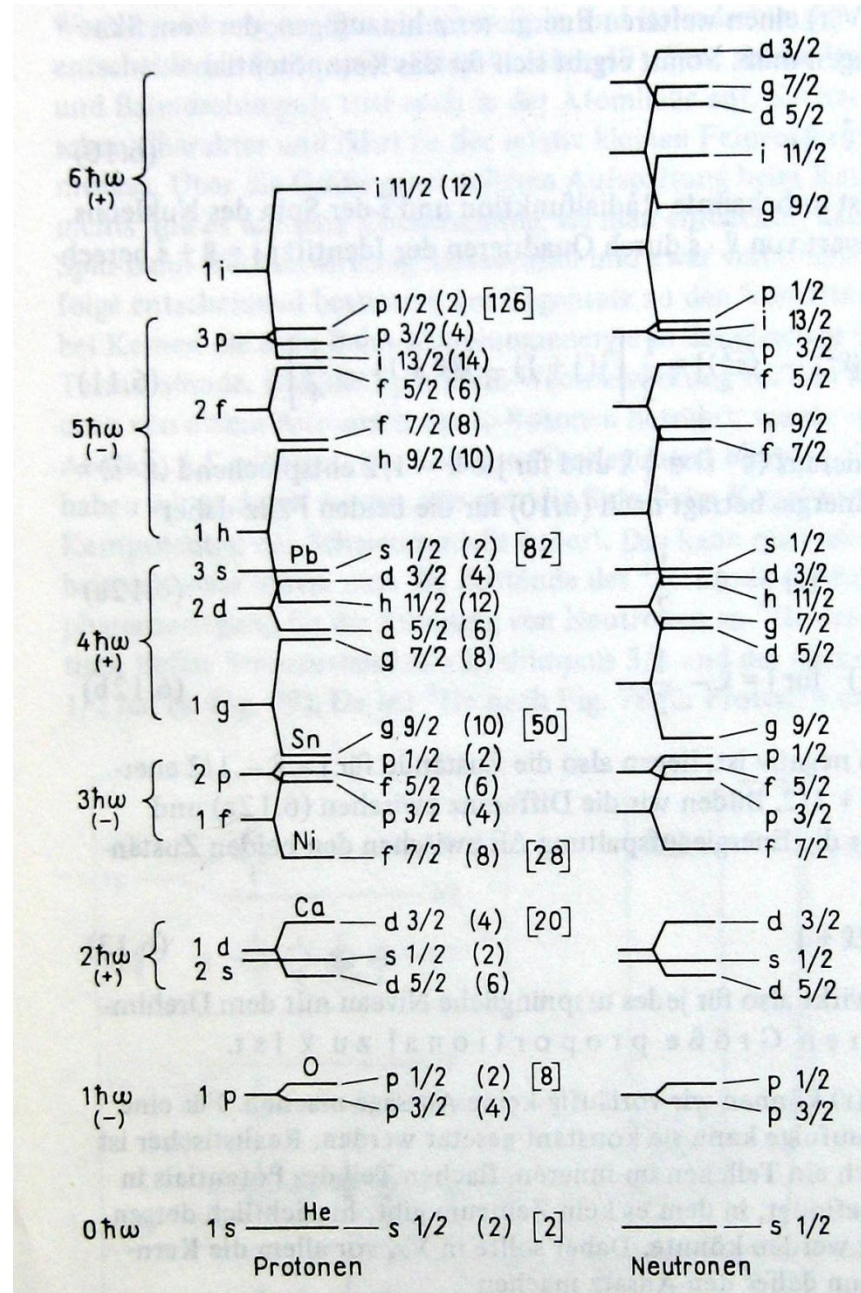
Also explains the magic numbers for divalent metals such as zinc or cadmium, at
4, 9, 10, 17, 20, 29 ... atoms.

$$2(2l + 1)$$

electrons

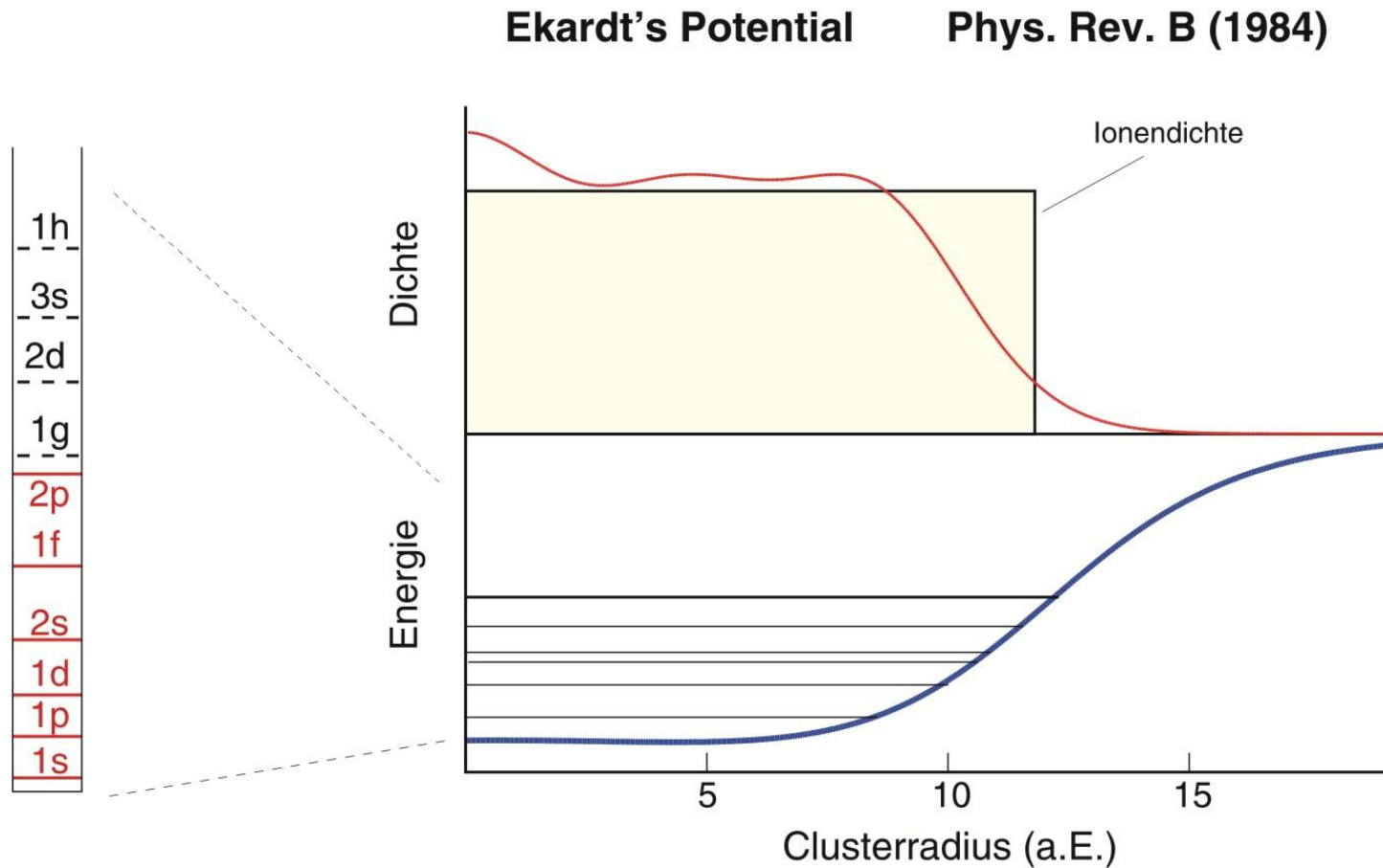
in the atomic nucleus:
 additional influence of
 spin-orbit interaction.

Can be neglected in
 clusters

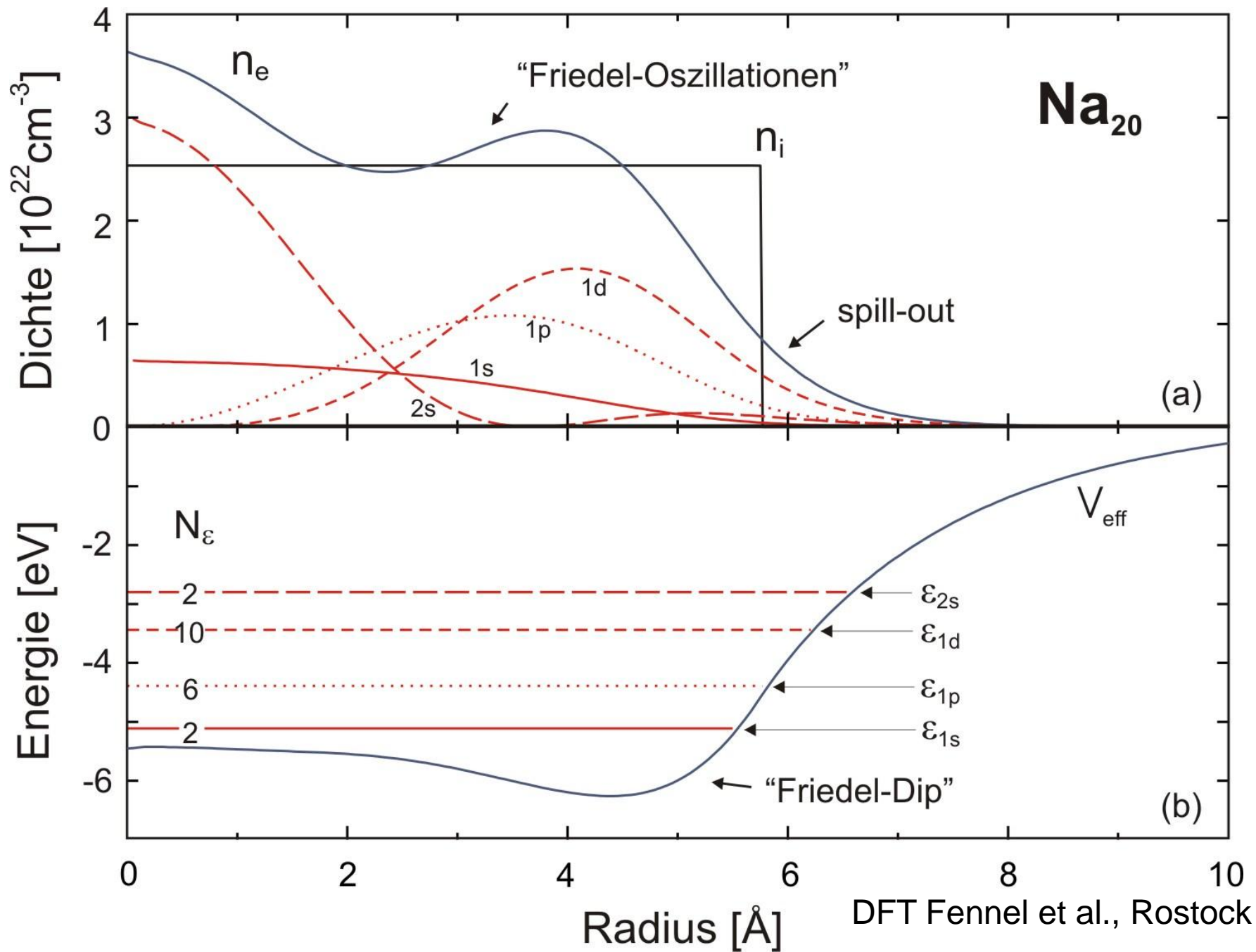


Mayer-Kuckuk

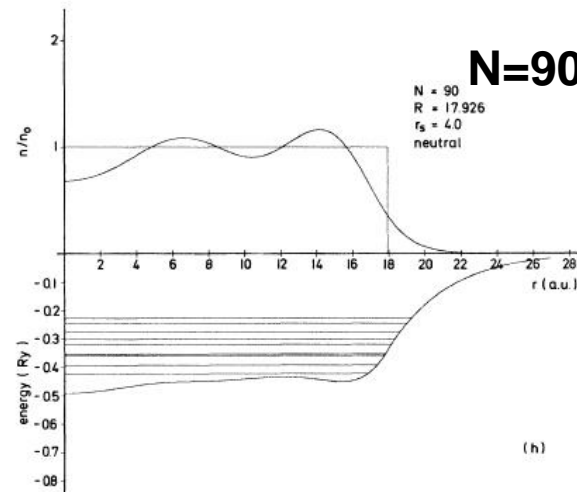
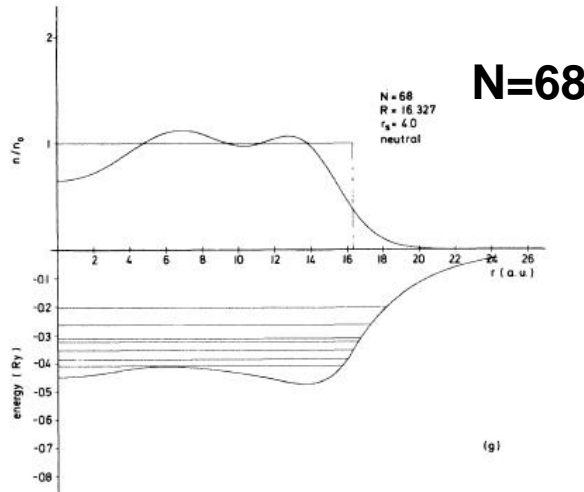
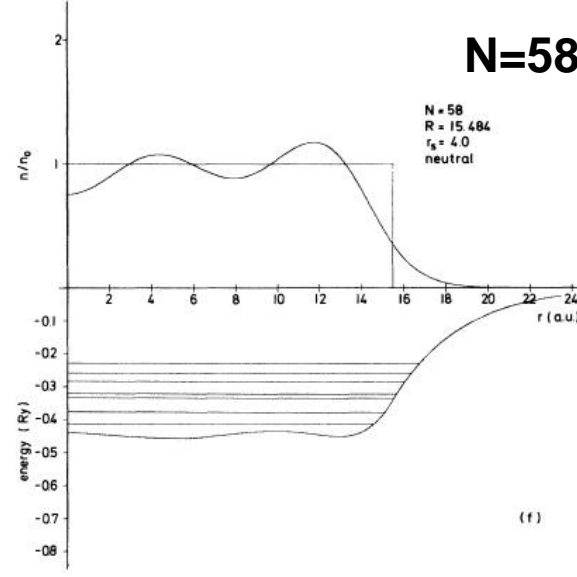
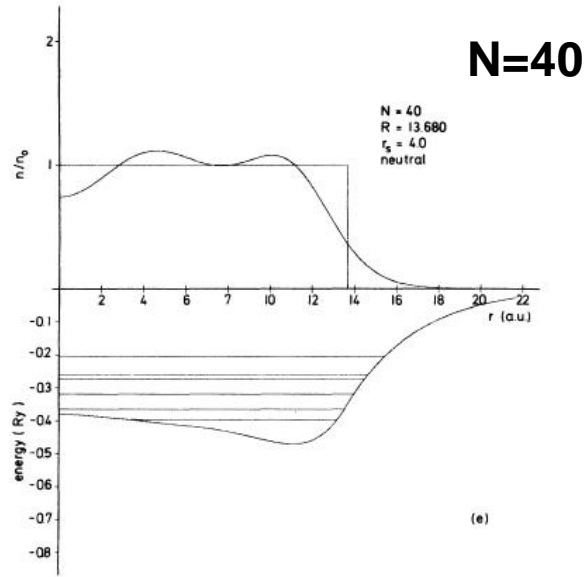
The jellium model for clusters: density functional theory



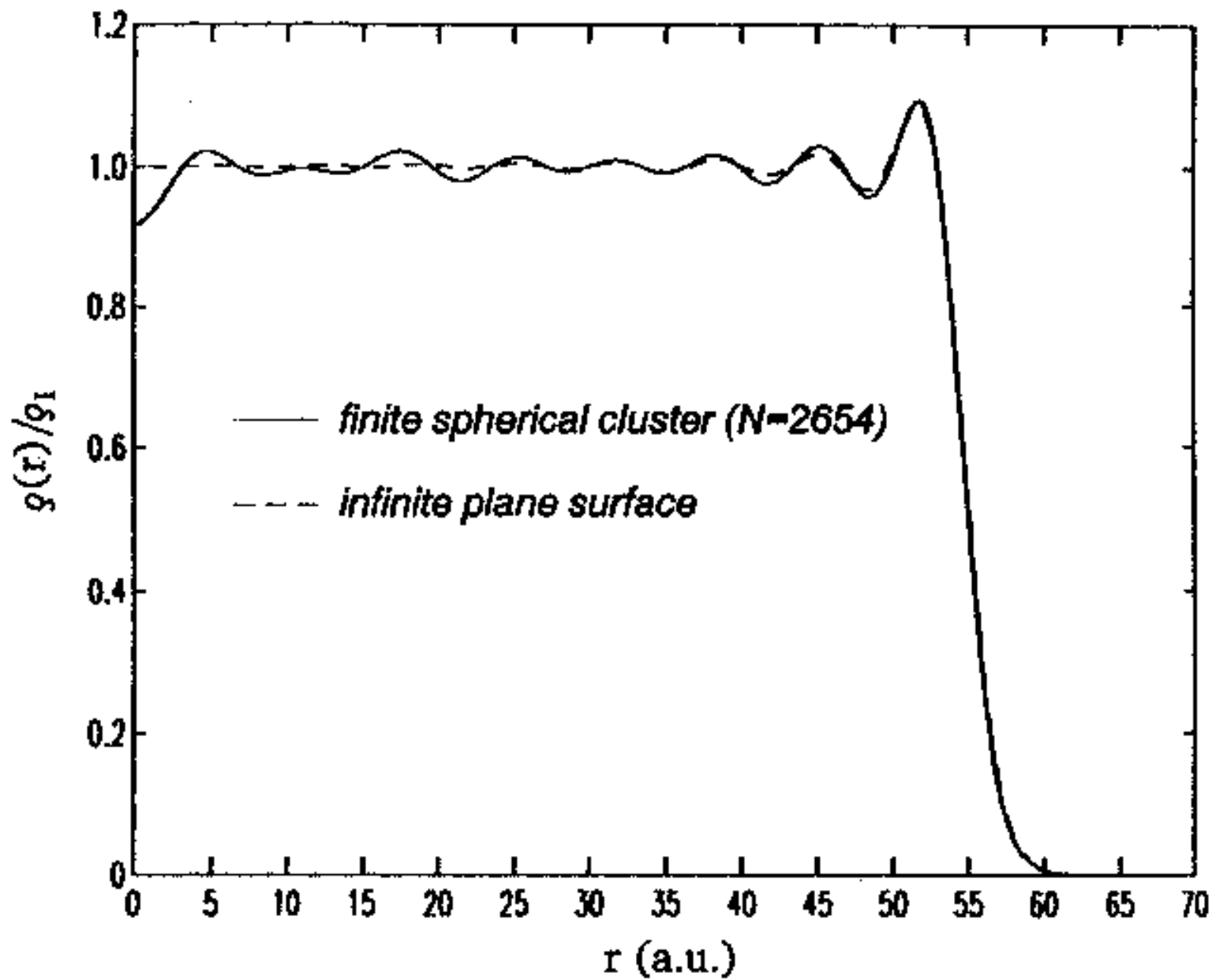
(Nearly) free electrons in a small volume. The electronic properties can either be described by a simple jellium model or more sophisticated by the density functional theory. In all cases the electron distribution extends over large parts of the jellium sphere. The corresponding eigenfunctions lead to the shell structure.



larger clusters:
self-consistent spherical jellium-background model



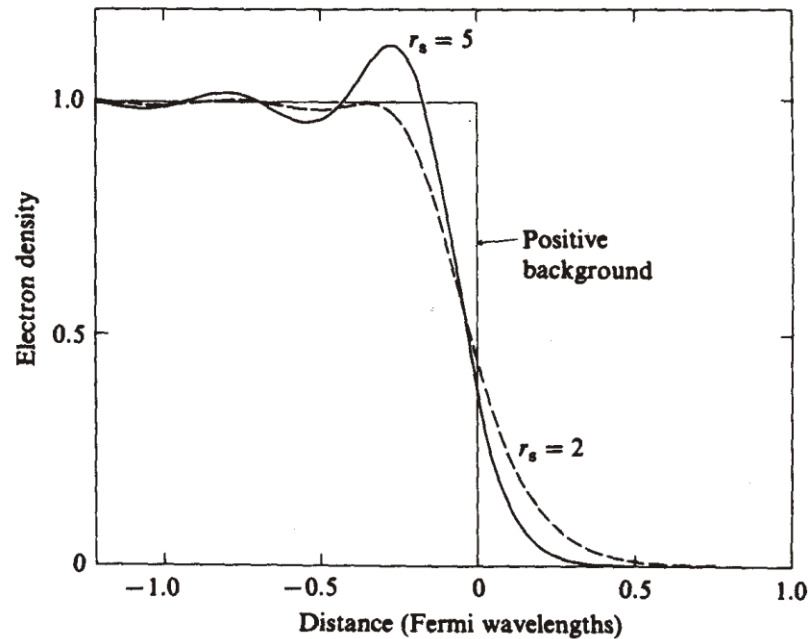
for very large clusters: close to bulk



compare: metal surfaces - resulting electron density

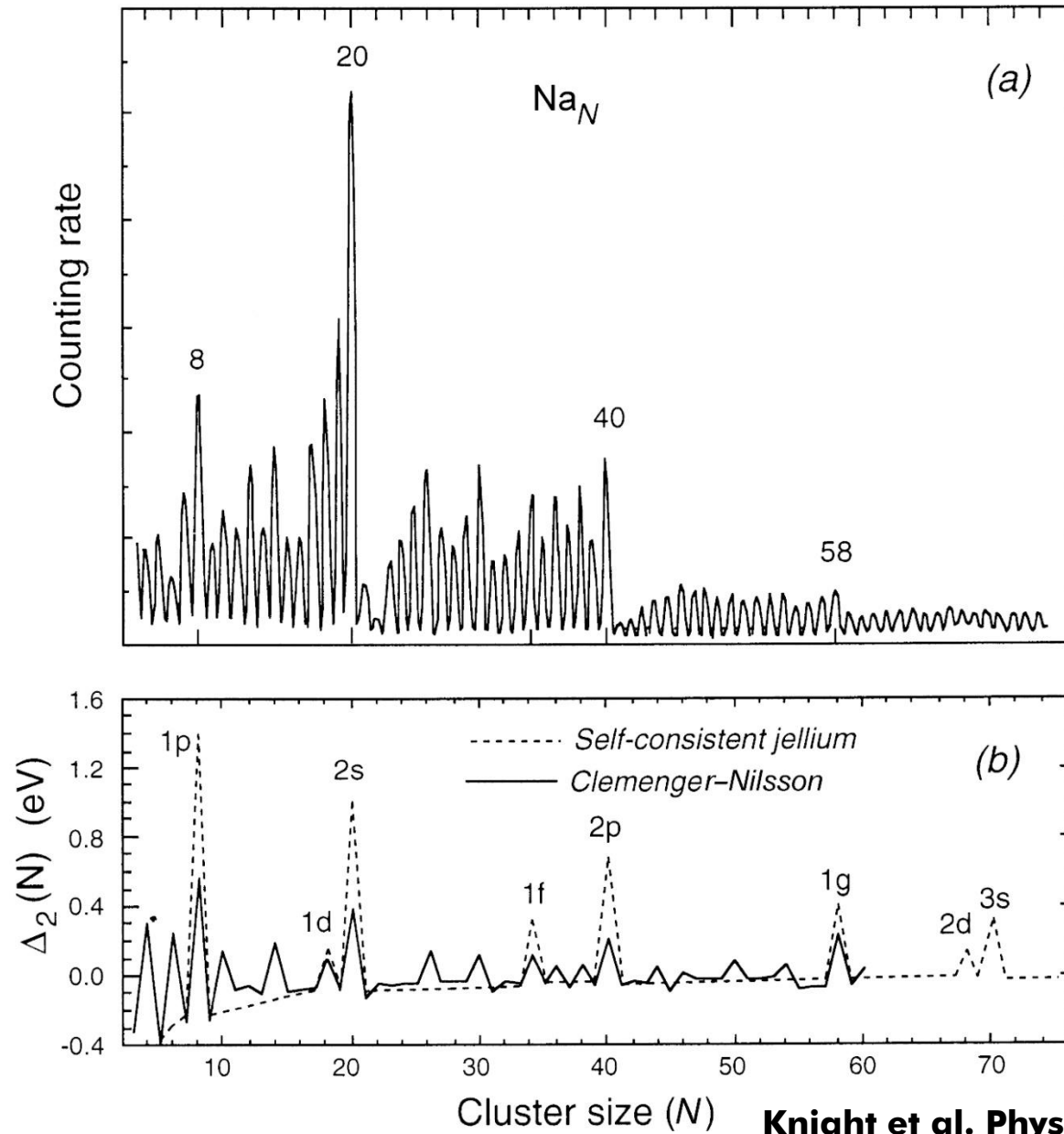
- electron density $n(z)$ shows oscillations (Friedel oscillations)
- $n(z)$ spills out beyond the ionic charge (electron spill-out)
- spill-out produces a surface dipole

Fig. 4.2. Electron density profile at a jellium surface for two choices of the background density, r_s (Lang & Kohn, 1970).

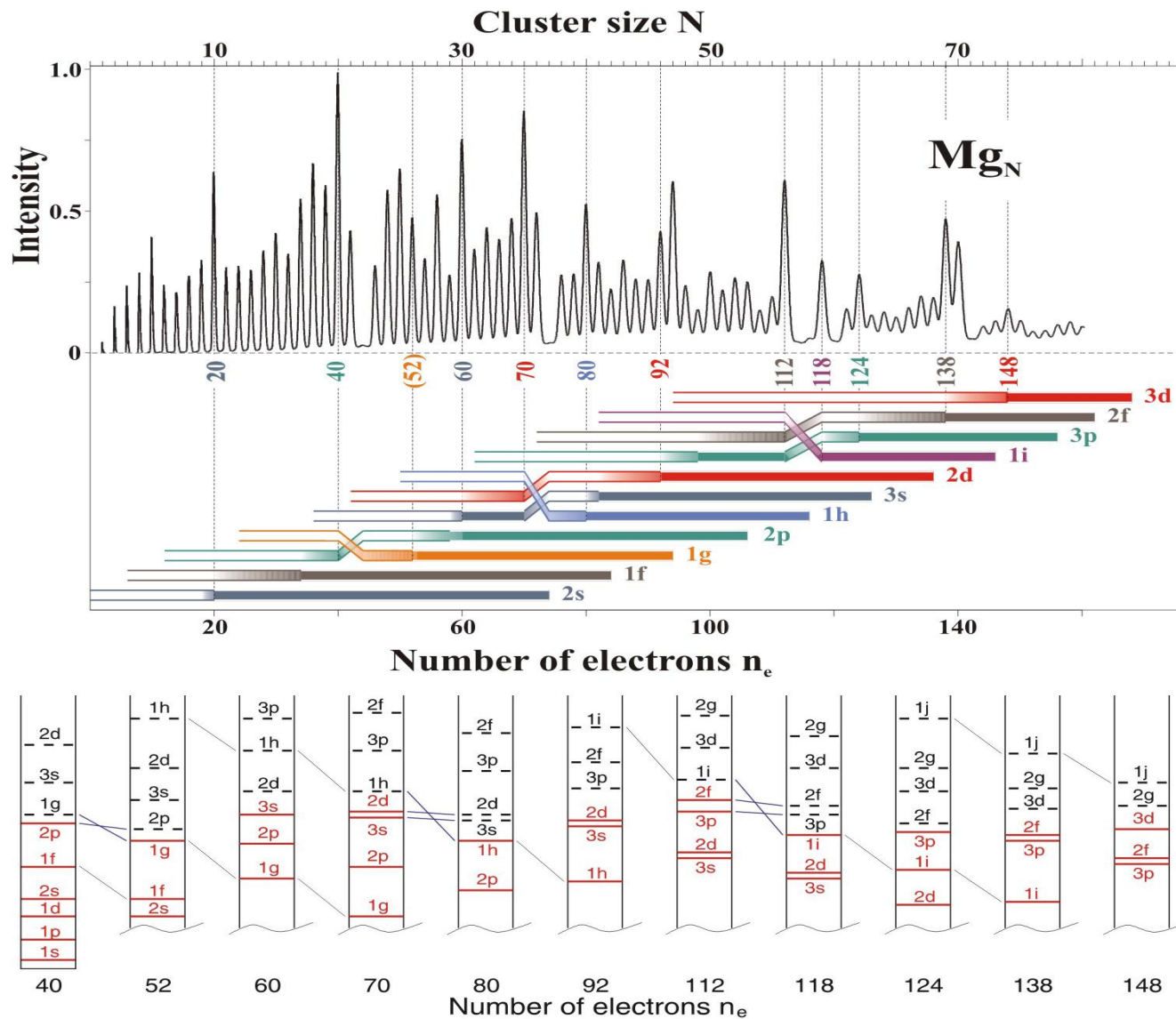


Ursache der Oszillation:
Elektronen mit festen Wellenvektor versuchen pos. Hintergrundladung abzuschirmen; hieraus folgen leichte Verschiebungen der einzelnen Atomlagen im Bereich der Oberfläche

jellium fingerprint in the mass spectra

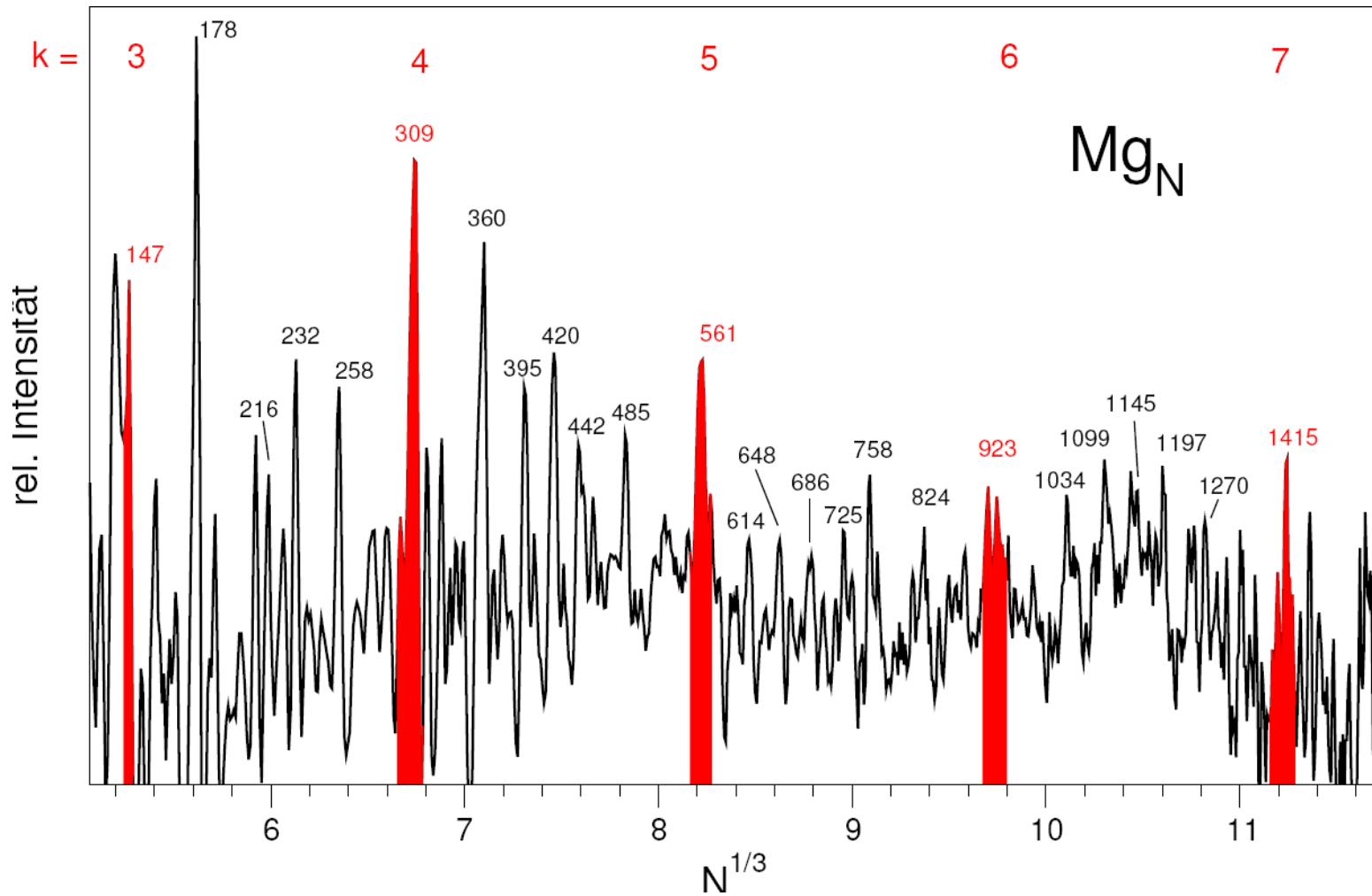


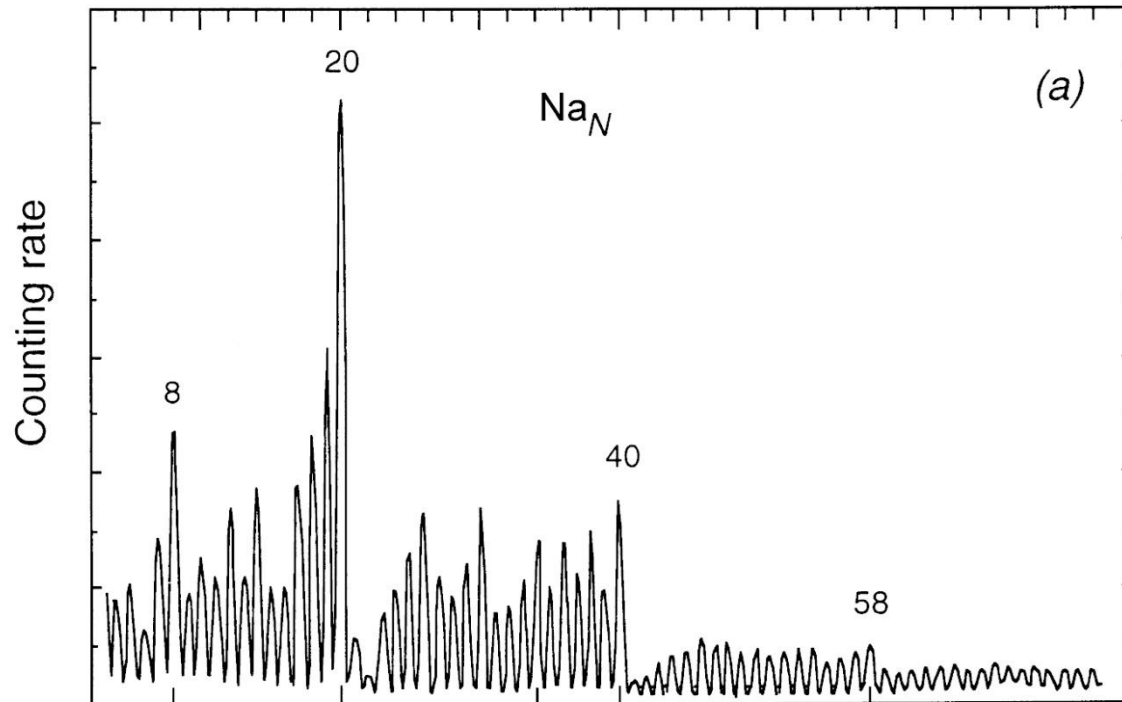
Small Magnesium clusters as another example for a jellium system.
 Now each atom contributes with two electrons



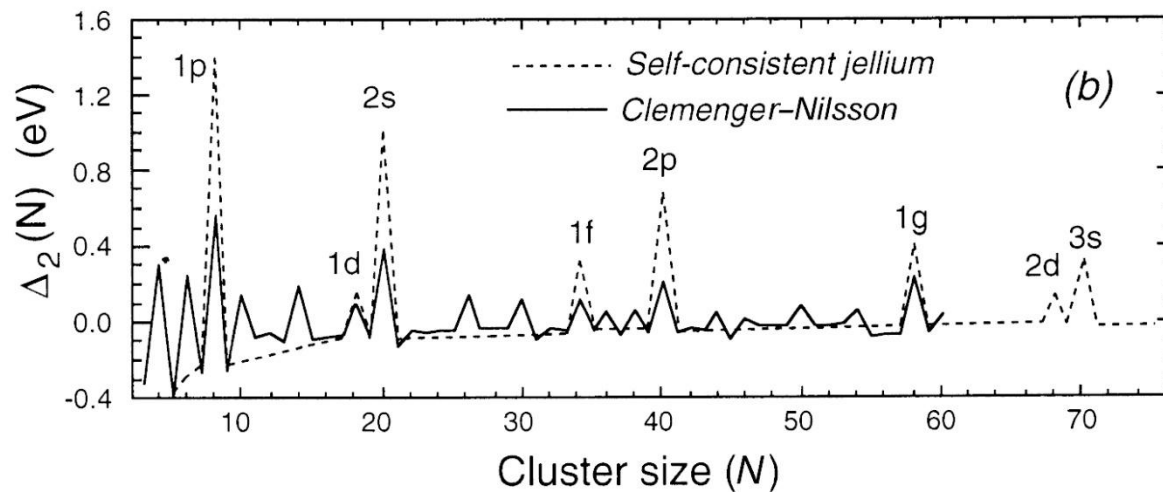
Electronic vs. geometrical shell

Example: large Mg_N



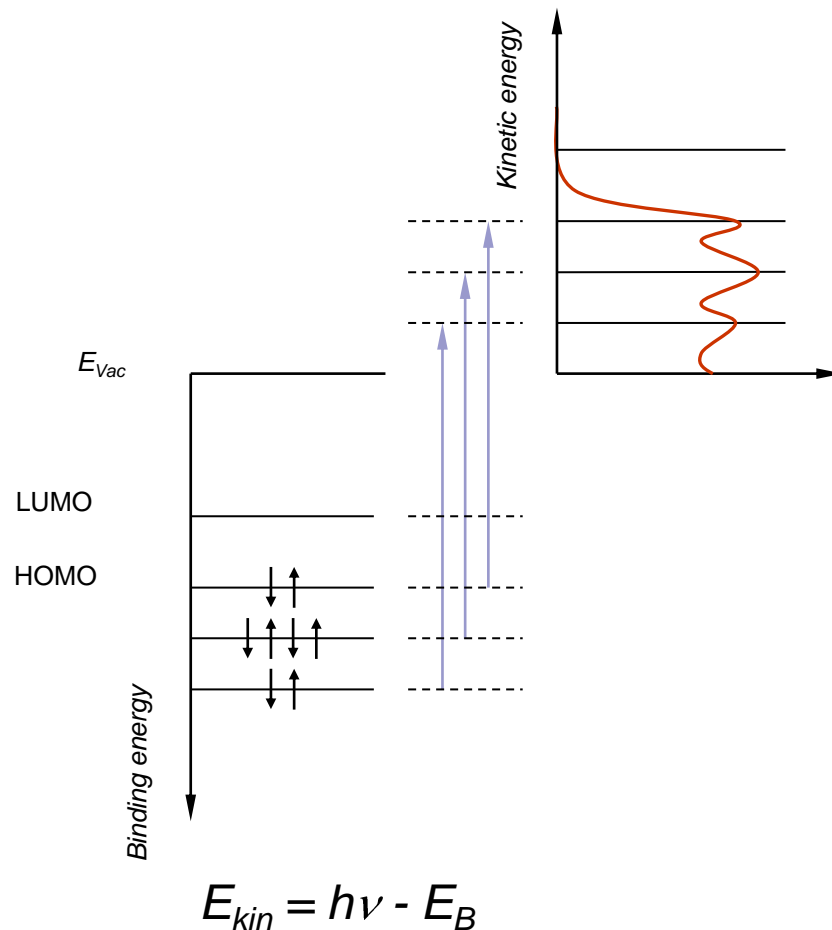


deformations explain
the sub-shell closings



Knight et al.

how to measure the electronic structure? by photoelectron spectroscopy



technical challenge: extremely low target density as it is necessary to work with a *charged* cluster beam. Only charged clusters can be mass selected

Magnetic bottle electron spectrometer

$$r_i = \frac{v \sin \theta_i}{\omega_i}, \quad \checkmark$$

$$\frac{\sin \theta_f}{\sin \theta_i} = \sqrt{\frac{B_f}{B_i}}$$

$$(2) \Rightarrow \frac{\Delta E}{E} \approx \frac{B_f}{B_i}$$

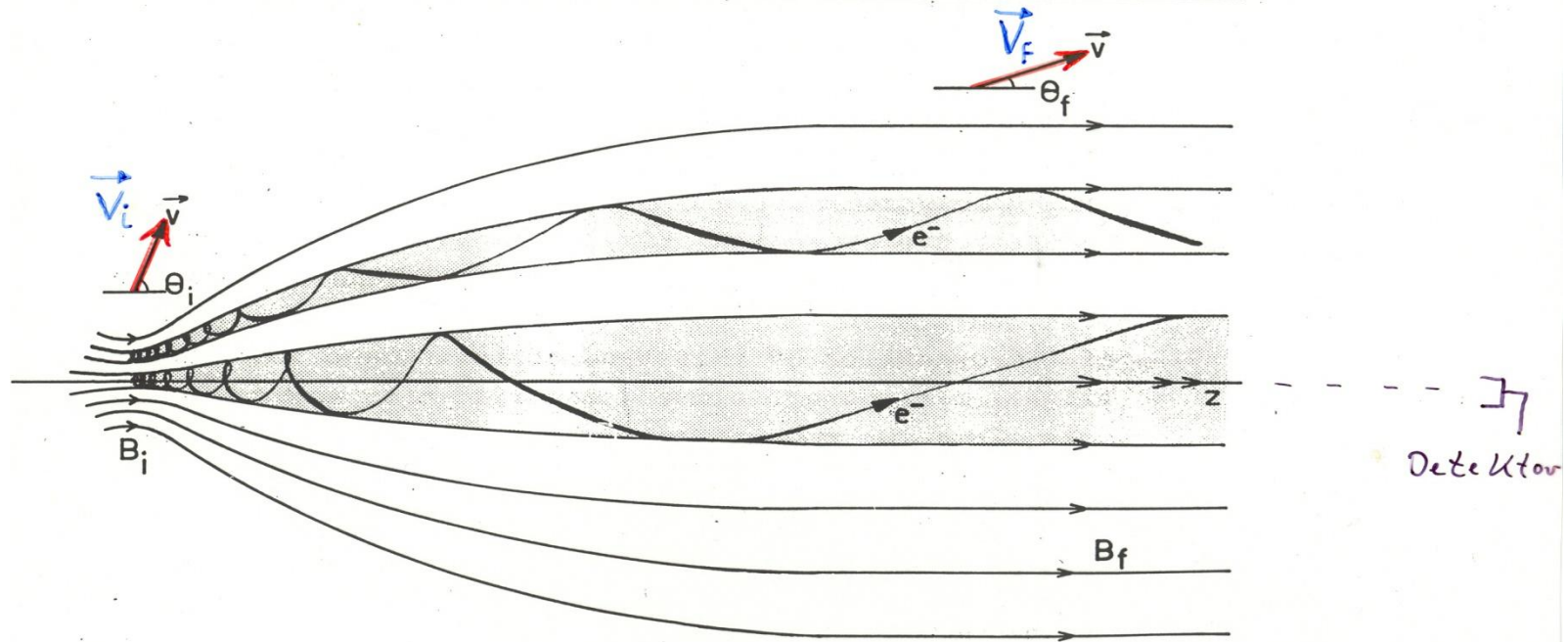


Figure 1

Schematic diagram showing the helical motion of an electron moving in a magnetic field that changes gradually from a strong field B_i to a weaker uniform field B_f .

Kruit, Read

in the limit of a strong gradient and a long drift area, the flight times of electrons with the same energy are independent of the emission angle.
detection efficiency of about 50 %

technical realization of a magnetic-bottle electron spectrometer

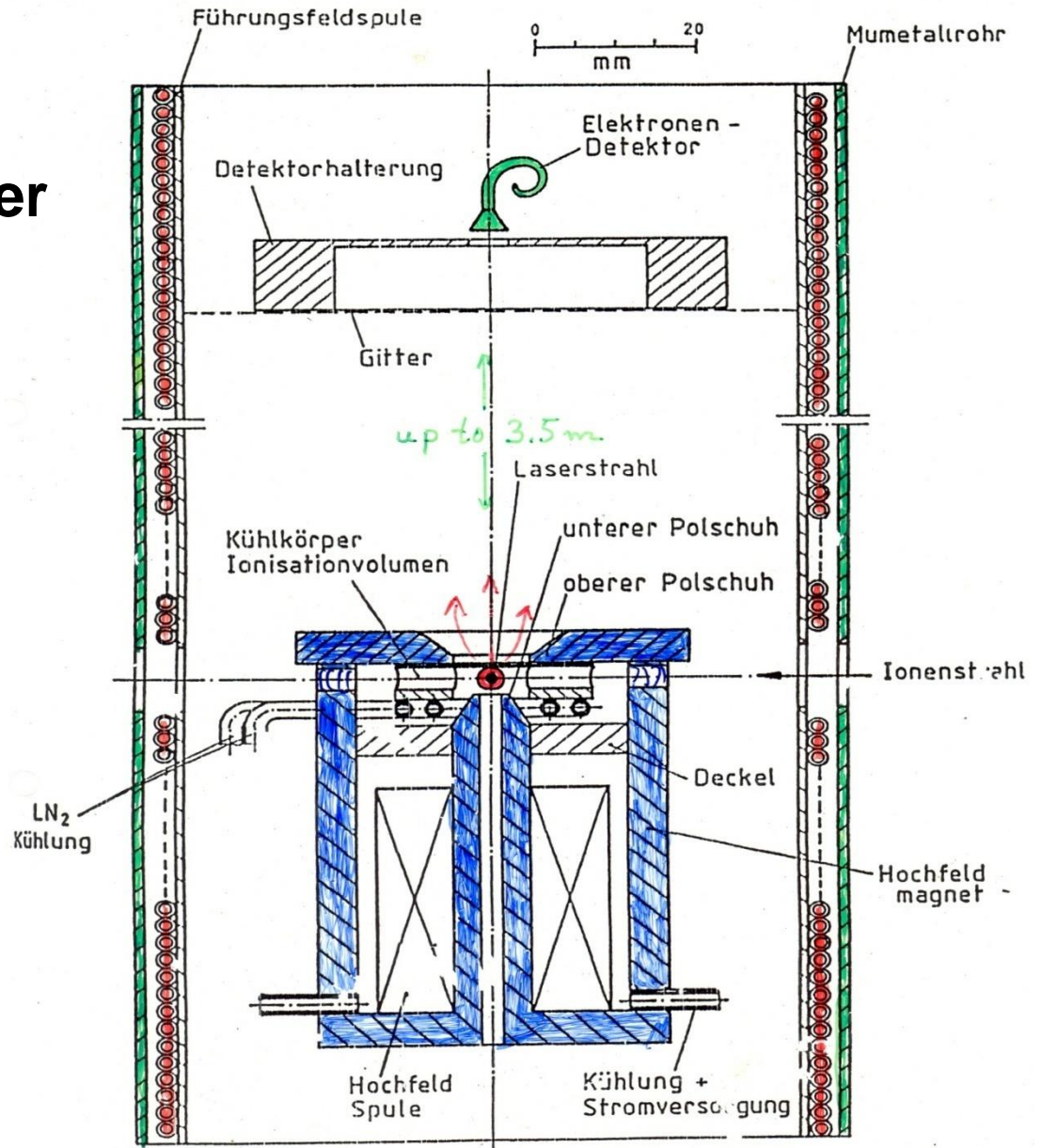
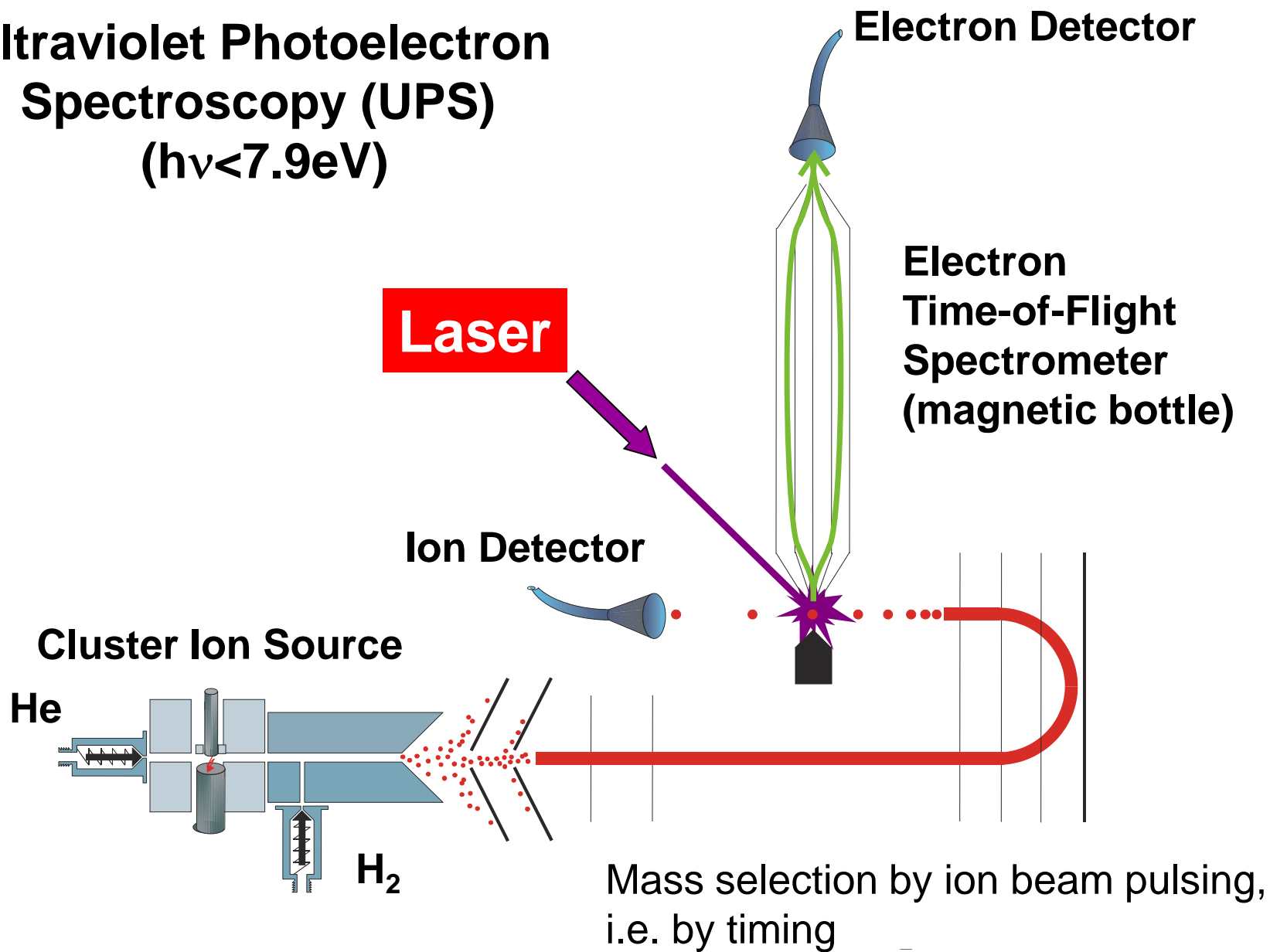


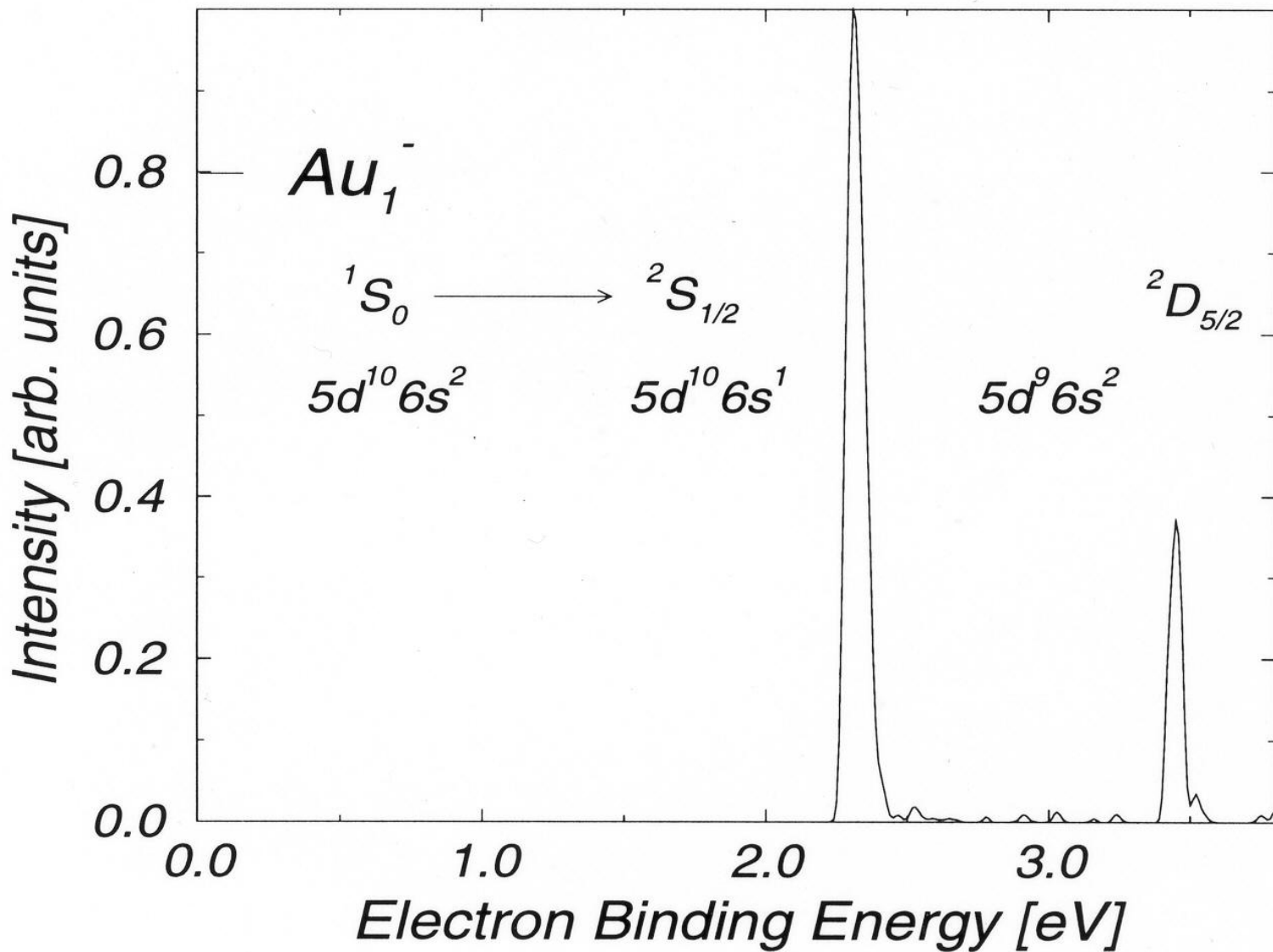
Abbildung 11: Schnitt durch den neuen Hochfeldmagneten

Ultraviolet Photoelectron Spectroscopy (UPS) ($h\nu < 7.9\text{eV}$)



Setup Ganteför group, Konstanz

Calibration mag. bottle spectrometer with Au₁⁻



Group Meiwes-Broer, Rostock

Photoelectron spectra from Ag_N^-

